Jordanian Journal of Computers and Information Technology (JJCIT), Vol. 08, No. 04, December 2022.

FEATURE LEVEL FUSION FRAMEWORK FOR BRAIN MR IMAGE CLASSIFICATION USING SUPERVISED DEEP LEARNING AND HAND CRAFTED FEATURES

Prashantha S. J.[1] and H. N. Prakash[2]

(Received: 16-Jun.-2022, Revised: 18-Aug.-2022, Accepted: 12-Sep.-2022)

ABSTRACT

In this paper, we propose an efficient fusion framework for brain magnetic resonance (MR) image classification using deep learning and handcrafted feature extraction methods; namely, histogram of oriented gradients (HOG) and local binary patterns (LBPs). The proposed framework aims to: (1) determine the optimal handcrafted features by Genetic Algorithm (GA) (2) discover the fully connected (FC) layers' features using fine-tuned convolutional neural network (CNN) (3) employ the canonical correlation analysis (CCA) and the discriminant correlation analysis (DCA) methods in feature-level fusion. Extensive experiments were conducted and the classification performance was demonstrated on three benchmark datasets; viz., RD-DB1, TCIA-IXI-DB2 and TWB-HM-DB3. Mean accuracy of 68.69%, 90.35% and 93.15% from CCA and 77.22%, 100.00% and 99.40% from DCA was achieved by the Support Vector Machines (SVM) sigmoid kernel classifier on RD-DB1, TCIA-IXI-DB2 and TWB-HM-DB3, respectively. The obtained results of the proposed framework outperform when compared with other state-of-the-art works.

KEYWORDS

Deep-learning features, Handcrafted features, Canonical-correlation analysis, Discriminant-correlation analysis, Support vector machines.

1. INTRODUCTION

A brain tumour is one of the most significant health problems in the human body. The accurate diagnosis and assessment of disease depend on computerized tools involved in diagnostic tasks. Computer-vision and machine-learning strategies promote early detection to identify the disorder of an individual based on imaging systems. In medical imaging, the acquisition and interpretation of images have improved substantially over recent years. Nowadays, magnetic-resonance imaging (MRI) is a widely used medical imaging method that assists in the detection of brain tumors [1]-[6]. The MRI scan gives detailed imaging information to distinguish cancerous structures from healthy ones, but it takes a long time to diagnose. Hence, to overcome this drawback, an automated approach is needed.

A typical pattern-recognition system consists of feature-extraction, selection and classification methods. Over the past decades, a large number of feature-extraction approaches have been developed, such as histogram of oriented gradients (HOG) [7], wavelet [3][8], convolutional neural network (CNN) [7], [9]-[11], Local Binary Patterns (LBPs) [12], …etc. On the other hand, feature selection uses several approaches, including ant-colony optimization (ACO), particle-swarm optimization (PSO), genetic algorithms (GAs) [13] [3] and so on. Sometimes, if we use more than one approach, neither a feature extraction nor selection can lead to multi-discriminatory features for the automated medical-diagnosis system. However, these multi-discrimination features hardly interact among themselves, which further limits their semantic relatedness. In this context, fusion methods are essential to generating rich features through fused representation in the automated system. In the process of fusion, the result can occur at the pixel level [14], feature level [15]-[16] and decision level [17] and that ensures the salient features that can improve recognition accuracy. Feature-level fusion has two advantages: first, it can eliminate redundant information between the cross-domain features; second, it may collect non-identical discriminatory features from different cross-domain feature sets.

Over the last few years, many research works on the MR brain-tumor diagnosis categorized brain imaging into two different types: (1) classifying the brain image as either abnormal or normal and (2)

1. Prashantha S. J. is with Department of Computer Science and Engneering, AIT Chikkamagaluru, Visvesvaraya Technological Uni., Belagavi, India. Email: prasi.sjp@gmail.com
2. H. N. Prakash is with Department of Computer Science and Engineering, RIT Hassan, Visvesvaraya Technological Uni., Belagavi, India. Email: prakash.hn98@gmail.com

classifying the abnormal brain image into various types of brain tumors. Kharrat et al. [3] proposed an automated diagnosis and classification approach for Magnetic Resonance (MR) human-brain images. This work used wavelet transform (WT) as an input-feature module to the Genetic Algorithm (GA) and Support Vector Machine (SVM). It separates MR brain images into normal and abnormal ones. Sethy P. K. and Behera S. K. [4] investigated the use of deep-classification methods with deep-learning features to identify tumorous brain MR images. They used the VGG19, VGG16 and Alex Net pre-trained network, combined with SVM for detecting the brain tumor using the 2D brain MRI slices. The work aim was to evaluate the performances of these methods. Ichrak Khoulqi and Najlae Idrissi [18], presented a method of pre-trained Deep Convolutional Neural Networks (DCNNs) based on Transfer Learning (TL) for cervical-cancer detection and classification using MRIs to classify the MRIs into two classes: benign or malign. In [19], the authors have introduced a novel technique for bias-field estimation and correction in MR images to enhance segmentation results. It comprises a modified expectation maximization clustering; the bias field is fitted as a hyper-surface in a 4D hyper-space.

The work proposed by H. H. Sultan et al. [20] classified different brain-tumor types by convolutional neural networks. The proposed method is comprised of two studies. The first study classifies tumors into different types; namely, meningioma, glioma and pituitary tumors. The second study is based on the differentiation between the three glioma grades. Saxena et al. [1] presented a study to classify brain MRI scans into two classes using Resnet-50, VGG-16 and Inception-V3 pre-trained models. However, the Inception-V3 model suffered from overfitting and is slightly better than a random classifier with an accuracy of 0.55. Moreover, the new state-of-the-art architectures are needed by using transfer-learning techniques to improve accuracy. S. Oreski & Oreski, G. [13] proposed a method to identify an optimum feature subset by the hybrid genetic algorithm with neural networks (HGA-NN). Chen et al. [21] proposed to address feature-selection problems through GAs for feature clustering, where a GA was used to optimize the cluster center values of a clustering method to group features into different clusters. Some of the researchers presented feature-level fusion to be more effective. The well-known (1) serial and (2) parallel methods are the most widely used in feature-fusion methods [15]. M. Haghighat et al. [16] presented the correlation analysis-based feature-set fusion for multi-modal biometric recognition. The method demonstrated the effectiveness in the fusion of feature sets extracted from a single modality. However, it uses the class associations of the samples by discriminant-correlation analysis (DCA).

The above-stated research works [1], [3]-[4], [20] have focused only on the identical feature type to build a classification approach of brain MR images. Hence, it is reasonable to propose a study of a multiple-feature fusion framework for brain MR-image classification task. In this work, we proposed an MR brain-image classification model based on a handcrafted and deep-feature fusion approach. The summary of this research work is as follows: (1)A novel proposed method including three significant steps: (i) Handcraft and deep-learning features are extracted from brain MR images, (ii) An optimal handcraft feature set is selected by a GA and (iii) Feature-level fusion operation is performed using CCA and DCA methods. (2) Conduction of experiments is extensively carried out on three benchmark datasets. (3) The robustness of the proposed strategy is evaluated.

In this paper, the contents of the research work are structured as follows. In Section 2, we proposed a novel feature-level fusion model that uses deep and handcrafted features to classify images as either normal or abnormal. In Section 3, experiments conducted are presented. We utilized three publicly available datasets and compared our work with five state-of-the-art works. In Section 4, a conclusion and future-work horizons are presented.

2. PROPOSED METHOD

Figure 1 describes the proposed method of feature-level fusion framework for brain MR-image classification. The methodology begins with a pre-processing step, in which the input brain MR-image is resized, normalized by the min-max method and enhanced by the bit-plane slicing method. Next, feature extraction and selection are done in two ways. First, local binary patterns (LBPs) and histogram of oriented gradients (HOG) methods as feature extractors and an optimal subset of features are determined by a Genetic Algorithm (GA), named as handcrafted features. Second, the fine-tuned CNN model acts as a feature extractor and selects deep features from two fully-connected layers (FC1

and FC2). Then, relevant features to the best-fitting feature space of a specific dimension are constructed using principal component analysis. The feature-level fusion techniques have been employed by DCA and CCA methods based on the combination of feature vectors. Finally, classification is performed using a support vector machine (SVM) classifier with a sigmoid function to recognize whether the given MR image is either normal or abnormal.

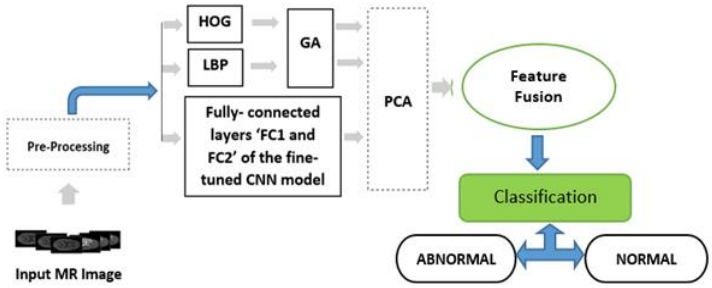

Figure 1. Architecture of the proposed methodology.

2.1 Pre-processing

Before classification, a pre-processing step is applied to MR brain images for the proposed methodology. All images are resized to 240x240 pixel dimensions using the bilinear method and image normalization is employed based on the min–max method. Meanwhile, the bit-plane slicing method [12] was applied, which determines whether a bit-plane contains significant information.

2.2 Feature Extraction and Selection

We extract the handcrafted (HOG and LBP) and fine-tuned CNN features. The HOG has to capture the edges and corners, whereas LBP has to identify the local micro-structure pattern. The HOG and LBP methods are applied for computing the features based on 32x32 cells, where 324 dimensions of HOG features and 531 dimensions of LBP features are obtained. We adapt a feature selection by Genetic Algorithm (GA) [3] to find the optimal handcrafted feature subset of HOG and LBP. But, despite that, fine-tuned CNN model is used as a trainable feature detector, which can extract low-level, high-level and highly adaptive features. We expand the CNN architecture of Fig.1 in the proposed framework described in Table 1. There are nine layers ordered as I, C1, P1, C2, P2, C3, P3, F1 and F2 in the sequence CNN model, where, I, C, P and F are denoted as the input, convolutional, pooling and fully connected layers, respectively. However, the architecture design of CNN was optimized using a trial and error approach. We extract layer-wise feature sets, out of which two fully connected layers (namely FC1and FC2) are deep-feature sets having 768 dimensions of richer high–level features obtained.

Table 1. Architecture of CNN.

Layer Name	Type of layer	Kernel size	Feature map
I	Input	-	240x240x1
C1	Conv1+ ReLU	5x5 , 32 filters	240x240x32
P1	Max- Pooling	2x2, stride 1	120x120x32
C2	Conv2+ ReLU	5x5 , 48 filters	120x120x48
P2	Max- Pooling	2x2, stride 1	60x60x32
C3	Conv3+ ReLU	5x5 , 64 filters	60x60x64
F1	Fully Connected (FC1) ReLU	1x384 -	1x384 1x384
F2	Fully Connected (FC2)	1x384	1x384

2.3 Fusion and Dimensionality Reduction

The feature-fusion process involves a high-feature space that is highly complicated. The proposed model uses handcrafted (HOG and LBP) and deep features of the fusion task. For this reason, the fusing of two or more inhomogeneous feature vectors leads to conflict. More features can allow for the chance of over-fitting. We used principal component analysis (PCA) to tackle the curse of dimensionality among HOG, LBP and deep features. The dimensionality-reduction process maps the

original predictor space to the best-fitting space of a specific dimension. Next, the fusion operation of an image by CCA and DCA methods is performed to determine the discrimination power on the future combinations.

2.4 Classification

In this work, we adopted the support vector machine (SVM) classifier for the automated brain MR-image classification. The CCA and DCA methods of feature fusion are used to train a binary-classification classifier. We used the sigmoid kernel function in the SVM algorithm. The classification results are evaluated and reported in terms of accuracy, sensitivity, specificity, precision, recall and F-measure metrics.

3. RESULTS

3.1 MR Dataset

The proposed method was applied and tested on three well-known, publicly available benchmark datasets. The acquisition protocol of each dataset includes T2- weighted MR images. The first dataset of brain MR images was downloaded from the radiopaedia.org website [22], labeled as RD-DB1. The RD-DB1 dataset comprises 100 images from 41 subjects or cases, out of which 50 images contain abnormalities and the remaining 50 images are normal. The second dataset was downloaded from The Cancer Imaging Archive (TCIA) [23] and IXI-dataset [24], named as TCIA-IXI-DB2. It comprises 200 images, out of which 50 for the TCGAGBM collection and 50 for the TCGA-LGG collection are tumors, while the remaining are from normal, healthy subjects in the IXI-dataset. The third dataset consists of 350 MR images from the Whole Brain Atlas-Harvard Medical School [25], designated as TWB-HM-DB3, which includes 140 abnormal and 210 normal images.

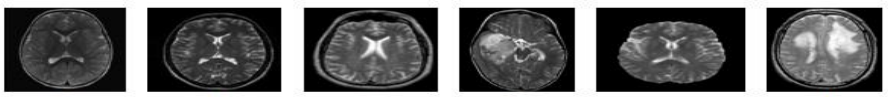

Figure 2. Sample of brain MR images: (a-c) Normal (d-f) Abnormal.

Figure 3. Results of the bit-plane method: (a-c) Normal (d-f) Abnormal.

3.2 Experimental Setup and Results

We conducted extensive experiments using three datasets of brain MR images. We used a bit-plane approach as pre-processing to provide feasible improvement. The bit-plane technique results are shown in Figure 3. We set up experiments based on composites of LBP, HOG and deep-feature vectors. The extraction of features was done from the two groups of image descriptors. The first group had two handcrafted features - the HOG and the LBP. The second group had the image feature representation learned by a fine-tuned CNN. Figure 4 shows the results of each handcrafted feature group. Meanwhile, original handcrafted features (HOG and LBP) are input to the Genetic Algorithm for feature selection, to determine the optimal features based on the fitness cost. Figure 5 shows the results of the best feature cost *versus* iteration plot by GA to select the optimal feature set. We used three datasets individually in this paper to select the k best significant features, including, (1) RD-DB1: The dataset consists of 41 cases with 100 images. Three features are extracted from these images. They are handcrafted LBP with dimension 142, HOG dimension 157 and deep features with dimension 768. (2) TCIA-IXI-DB2: The dataset contains 200 images. The three features extracted are: LBP with dimension 153, HOG with dimension 157 and 768 dimensions of deep features and (3) TWB-HM-DB3: The dataset contains 350 images. Both handcrafted and deep features are extracted from these images. They are HOG with dimension 161, LBP with dimension 146 and deep-learning features with dimension 768. To eliminate bias induced by unequal dimensions of feature groups, we utilize PCA to lower the dimensions of the features on a group-by-group basis.

Jordanian Journal of Computers and Information Technology (JJCIT), Vol. 08, No. 04, December 2022.

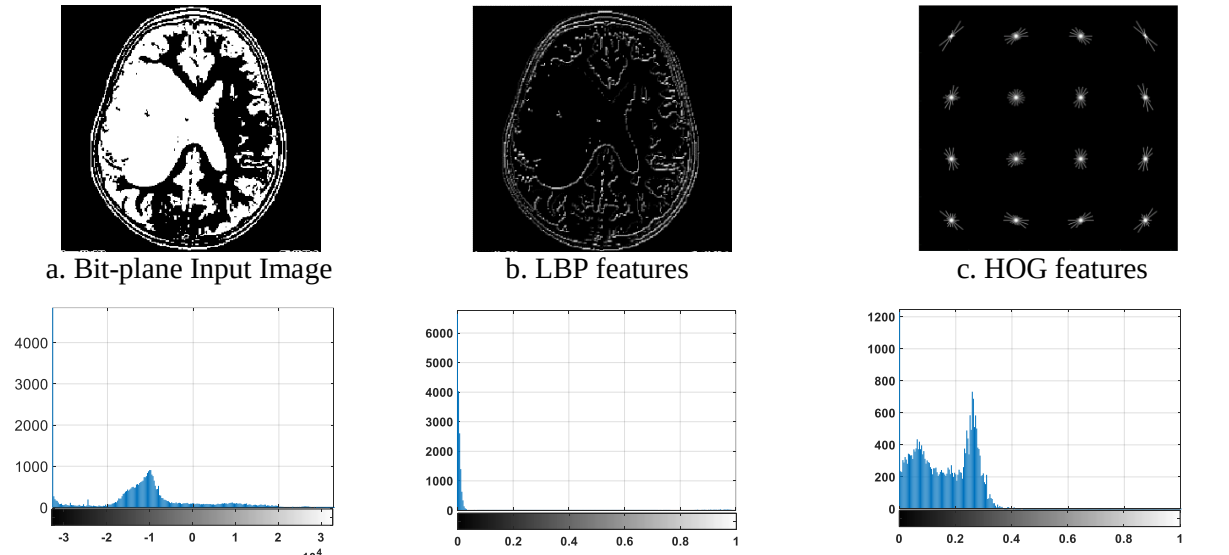

a. Bit-plane Input Image b. LBP features c. HOG features

d. Histogram of Image features e. Histogram of LBP features f. Histogram of HOG features

Figure 4. Results of feature extraction.

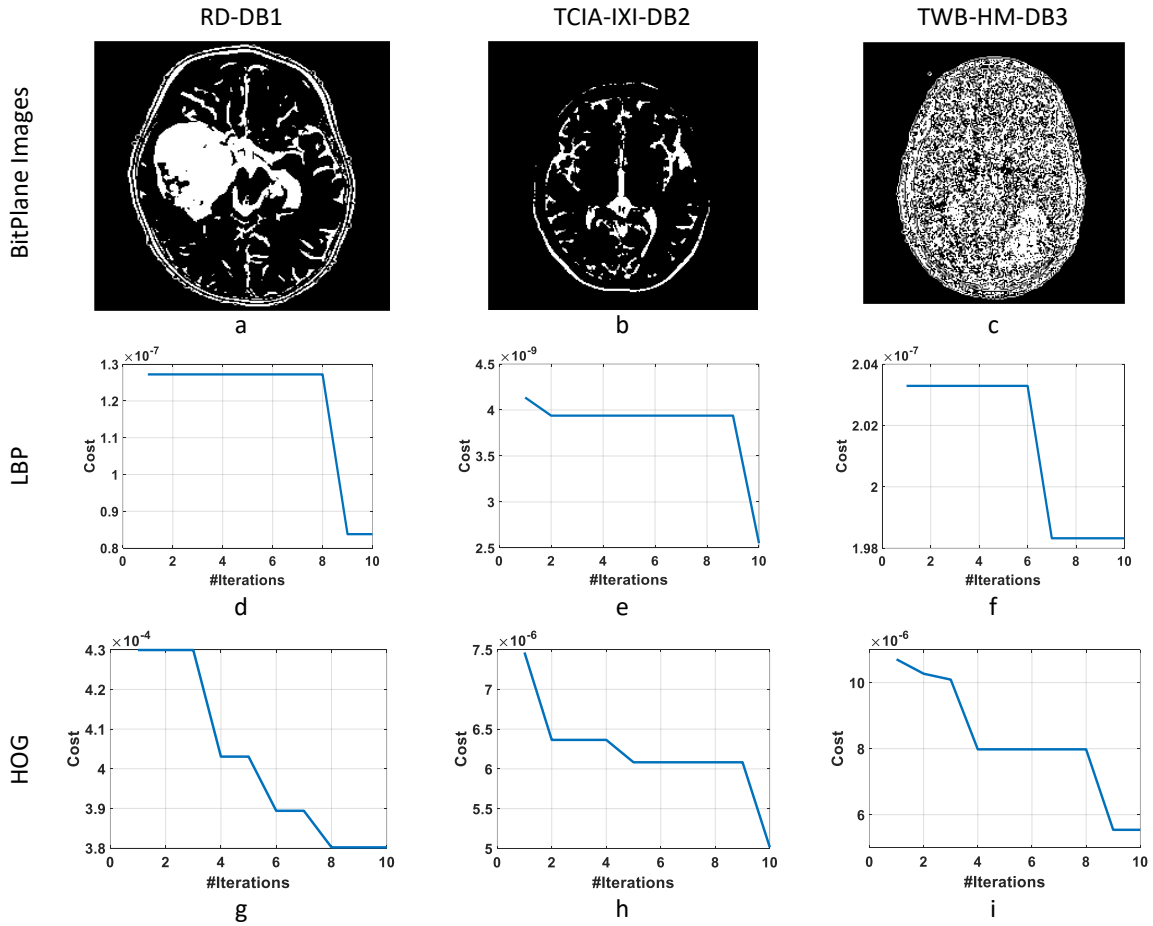

Figure 5. Feature-selection results of (a-c) Bit-plane images (d-f) LBP and (g-i) HOG feature best cost plot by GA.

Figure 4a and Figure 4d demonstrate the bit-plane input image and histogram of image features. Bit-plane slicing is a method of representing an image with one or more bits of the byte used for each pixel. It is converting a gray-level image into a binary image, making the informative region and the noise-like region. Figure 4b and Figure 4e, show an example of computing and visualizing a full LBP 2D array. LBP is a texture descriptor used for the property of high discrimination power. LBP labels each pixel in an image by comparing the gray level with the neighboring pixels and then assigning a

binary number. Finally, using histograms, we represent the frequency of LBP pattern that occurs in the image. In Figure 4c and Figure 4f, we clearly visualize the parts that have strong HOG features of the brain. The HOG feature focuses on the structure or the shape of an object. For the regions of the image, it generates histograms using the magnitude and orientation of the gradient to compute the features as a HOG-feature vector.

3.3 Discussion

The classification result for each dataset is based on a training set (70%, 80% and 90% of the total dataset) and a testing set (30%, 20% and 10% of the total dataset). An appropriate classifier is required to test the performance of the proposed classification method. In this approach, we use SVM with sigmoid kernel classifier in the recognition of brain images. During testing, the confusion matrix displays the classification results [26]. Here, TP (True Positive): correctly classified abnormal or positive cases; TN (True Negative): correctly classified normal or negative cases; FP (False Positive): incorrectly classified normal or negative cases; FN (False Negative): incorrectly classified abnormal or positive cases. We used mean accuracy, sensitivity, specificity, precision, recall and F-measure as evaluation metrics. The results in terms of average accuracy over all 3 datasets of test images are shown in Table 2. The proposed-approach fusion-performance results with respect to different metrics are shown in Table 3 and Table 4.

Table 2. Performance results by SVM classifier.

Feature combination HOG/LBP/DL	**RD-DB1**		**TCIA-IXI-DB2**		**TWB-HM-DB3**	
	CCA	**DCA**	**CCA**	**DCA**	**CCA**	**DCA**
	Acc (%)	**Acc (%)**	**Acc (%)**	**Acc (%)**	**Acc (%)**	**Acc (%)**
LBP+HOG	68.89	77.78	91.27	100.00	95.74	100.00
LBP+DL	70.56	76.11	92.00	100.00	95.45	98.21
HOG+DL	66.67	77.77	87.78	100.00	89.87	100.00
Average	68.70	77.22	90.35	100.00	93.67	99.40

Acc: Accuracy.

Table 3. CCA-based fusion-performance results.

Dataset	**Feature Type**	**Sensitivity**	**Specificity**	**Precision**	**Recall**	**F-measure**
RD-DB1	LBP+HOG	0.6793	0.7041	0.7111	0.6793	0.6930
	LBP+DL	0.7079	0.7129	0.7222	0.7079	0.7099
	HOG+DL	0.6627	0.6718	0.7222	0.6627	0.6883
TCIA-IXI-DB2	LBP+HOG	0.8764	0.9335	0.9389	0.8764	0.9064
	LBP+DL	0.9222	0.9222	0.9222	0.9222	0.9222
	HOG+DL	0.8757	0.8818	0.8889	0.8757	0.8816
TWB-HM-DB3	LBP+HOG	0.9087	0.9277	0.9574	0.9418	0.9418
	LBP+DL	0.9027	0.9277	0.9545	0.9405	0.9405
	HOG+DL	0.9320	0.8632	0.8944	0.9320	0.9111

Table 4. DCA-based fusion-performance results.

Dataset	**Feature Type**	**Sensitivity**	**Specificity**	**Precision**	**Recall**	**F-measure**
RD-DB1	LBP+HOG	0.8412	0.7589	0.7333	0.8412	0.7683
	LBP+DL	0.6934	0.9722	0.9777	0.6934	0.8075
	HOG+DL	0.7936	0.8677	0.8444	0.7936	0.7870
TCIA-IXI-DB2	LBP+HOG	1	1	1	1	1
	LBP+DL	1	1	1	1	1
	HOG+DL	1	1	1	1	1
TWB-HM-DB3	LBP+HOG	1	1	1	1	1
	LBP+DL	0.9705	1	1	0.9705	0.9850
	HOG+DL	1	1	1	1	1

The outcomes of experiments revealed a greater discriminative feature in all cases. The proposed CCA-based and DCA-based feature-fusion approaches perform extremely well in various feature vectors together. This might be because these approaches reduce the amount of redundant information in the two input-feature vectors. Surprisingly, the proposed method stipulates a more powerful feature vector from CCA and DCA-based fusion frameworks for the classification target. We sent all the three dataset images separately to a classifier and then recorded the computation time of training and testing. The average computation time consumed by our proposed system with RD-DB1 of classification in CCA is about 0.571 s (training), 0.010s (testing) and for DCA is about 0.574 s (training), 0.012 s (testing). The training time of TCIA-IXI-DB2 is about 0.58s by CCA and 0.57s by DCA, testing time is about 0.014s in CCA and 0.013s in DCA. Furthermore, in TWB-HM-DB3, the classification time is 0.58s (training), 0.015s (testing) in CCA, while in DCA, it is 0.601s (training), 0.013s (testing).

3.4 Comparative Analyses

In this sub-section, we compare the results of the proposed model to those of other state-of-the-art models of MR brain-image classification. So, our intention is to present at this point the results reported in the works [1], [3]-[6] along with the obtained results in the proposed model. In practice, the classification of brain-tumor MR images is done in two ways. The first way is to identify whether the brain MR images are normal or abnormal. The second way is to classify abnormal brain MR images into different tumor types. Table 5 compiles the best (highest) accuracy reported for different approaches. We say that we did not implement or test the other models, but we present the best results of those existing in [1], [3]-[6]. Subsequently, the comparison reveals that the application of the proposed approach directly to the projected fusion features shows improved performance when compared to the original features. However, the efficiency of our model remains higher than those of several previous state-of-the-art works.

Table 5. Performance comparison with state-of-the-art methods.

Study	Feature Extraction	Classification Method	Number of MR Images	Accuracy
Saxena et al., 2019 [1]	CNN	CNN with transfer learning	253	95.00%
Kharrat et al., 2010 [3]	Wavelet-based features	Genetic algorithm with SVM	83	98.14%
Ullah et al., 2020 [4]	DWT	Feed-forward neural network	71	95.80%
B. Ural, 2018 [5]	KMFCM	Probabilistic neural network	25	90.00%
Hemanth et al., 2019[6]	CNN	CNN	220	94.50%
Proposed method (CCA)	HOG+LBP+DL	SVM	100	68.69%,
Proposed method (CCA)	HOG+LBP+DL	SVM	200	90.35%
Proposed method (CCA)	HOG+LBP+DL	SVM	350	93.15%,
Proposed method (DCA)	HOG+LBP+DL	SVM	100	77.22%
Proposed method (DCA)	HOG+LBP+DL	SVM	200	100.00%
Proposed method (DCA)	HOG+LBP+DL	SVM	350	99.40%

Table 5 describes the comparison results of the proposed classification method with state-of-the-art methods. It is clear that the proposed structure gives better prediction results compared to structures given in other related previous studies, which demonstrates the reliability of the proposed model. In contrast, Saxena et al. [1] used feature engineering to extract features and then reduced their dimensions to use them in another stage for classification. In [3], genetic algorithm with SVM was used as a classification method based on wavelet features and achieved 98.14% accuracy; however, the model involves less number of MR images. In [4]-[6], the authors used pathological images to train the network, using DWT, KMFCM and CNN feature-extraction methods with less accuracy.

4. CONCLUSION

In this work, we have presented a brain MR-image classification approach jointly using deep and handcrafted features to classify images as either normal or abnormal. The approach has been used for T2-weighted brain MR images only. We made a successful attempt and explored the applicability of correlation analysis to two groups of features. We found that HOG, LBP and deep features are complementary for image representation and that two or more features are better than a single one. The main limitation of feature-extraction models was the high dimensions of features. However, we addressed this issue with PCA-based dimension reduction. We introduced the canonical and discrimination-correlation analysis of fusion features and achieved very good average-classification rates. The effectiveness of the proposed classification system is validated through well-known measures. In future work, we will explore further improvements in the classification approach with symbolic-representation schemes and better ways to handle more features.

ACKNOWLEDGEMENTS

The authors would like to thank all anonymous reviewers for their valuable suggestions to improve the quality of the research paper.

REFERENCES

[1] P. Saxena, A. Maheshwri, S. Tayal and S. Maheshwari, "Predictive Modeling of Brain Tumor : A Deep Learning Approach," Innovations in Computational Intelligence and Computer Vision, Part of the Advances in Intelligent Systems and Computing Book Series, vol. 1189, pp. 275–285, 2019.

[2] H. M. Rai and K. Chatterjee, "Detection of Brain Abnormality by a Novel Lu-Net Deep Neural CNN Model from MR Images," Machine Learning with Applications, vol. 2, p. 100004, 2020, DOI: 10.1016/j.mlwa.2020.100004, 2020.

[3] A. Kharrat, K. Gasmi and M. B. E. N. Messaoud, "A Hybrid Approach for Automatic Classification of Brain MRI Using Genetic Algorithm and Support Vector Machine," Leonardo Journal of Sciences, vol. 17, pp. 71–82, 2010.

[4] Z. Ullah, M. Umar, S. Lee and D. An, "A Hybrid Image Enhancement Based Brain MRI Images Classification Technique," Medical Hypotheses, vol. 143, no. May, p. 109922, 2020.

[5] B. Ural, "A Computer-based Brain Tumor Detection Approach with Advanced Image Processing and Probabilistic Neural Network Methods," J. of Medical Biological Eng., vol. 38, pp. 867–879, 2018.

[6] D. J. Hemanth, J. Anitha, A. Naaji, O. Geman, D. E. Popescu and L. H. Son, "A Modified Deep Convolutional Neural Network for Abnormal Brain Image Classification," IEEE Access, vol. 7, pp. 4275-4283, DOI: 10.1109/ACCESS.2018.2885639, 2018.

[7] T. J. Alhindi, S. Kalra, K. H. Ng, A. Afrin and H. R. Tizhoosh, "Comparing LBP , HOG and Deep Features for Classification of Histopathology Images," Proc. of the 2018 IEEE Int. Joint Conf. on Neural Networks (IJCNN), DOI: 10.1109/IJCNN.2018.8489329, Rio de Janeiro, Brazil, 2018.

[8] P. K. Sethy and S. K. Behera, "A Data Constrained Approach for Brain Tumour Detection Using Fused Deep Features and SVM," Multimedia Tools and Applications, vol. 80, no. 19, pp. 28745–28760, 2021.

[9] B. Athiwaratkun and K. Kang, "Feature Representation in Convolutional Neural Networks," arXiv: 1507.02313, pp. 6–11, 2015.

[10] N. Tajbakhsh et al., "Convolutional Neural Networks for Medical Image Analysis: Fine Tuning or Full Training ?" IEEE Trans. on Medical Imaging, vol. 35, no. 5, pp. 1299–1312, 2016.

[11] Z. Zhou, J. Shin, L. Zhang, S. Gurudu, M. Gotway and J. Liang, "Fine-tuning Convolutional Neural Networks for Biomedical Image Analysis," Proc. of the 2017 IEEE Conf. on Computer Vision and Pattern Recognition (CVPR), pp. 4761–4772, DOI: 10.1109/CVPR.2017.506, Honolulu, USA, 2017.

[12] S. Maheshwaria, V. Kanhangada, R. Pachoria, B. Sulatha V. and U. R. Acharyac, "Automated Glaucoma Diagnosis Using Bit-plane Slicing and Local Binary Pattern Techniques," Computers in Biology Medicine, vol. 105, pp. 72–80, 2019.

[13] S. Oreski and G. Oreski, "Expert Systems with Applications Genetic Algorithm-based Heuristic for Feature Selection in Credit Risk Assessment," Expert Systems with Applications, vol. 41, no. 4-2, pp. 2052-2064, 2013.

[14] S. Li, X. Kang, L. Fang, J. Hu and H. Yin, "Pixel-level Image Fusion: A Survey of the State of the art," Information Fusion, vol. 33, pp. 100–112, DOI: 10.1016/j.inffus.2016.05.004, 2016.

[15] J. Yang, J. Y. Yang, D. Zhang and J. F. Lu, "Feature Fusion: Parallel Strategy *vs.* Serial Strategy," Pattern Recognition, vol. 36, no. 6, pp. 1369–1381, 2003.

[16] M. Haghighat, M. Abdel-Mottaleb and W. Alhalabi, "Discriminant Correlation Analysis: Real-time

Feature Level Fusion for Multimodal Biometric," IEEE Transactions on Information Forensics and Security, vol. 11, no. 9, pp. 1984 - 1996, 2016.
[17] S. Roheda and H. Krim, "Decision Level Fusion : An Event Driven Approach," Proc. of the 26th IEEE European Signal Processing Conf. (EUSIPCO), vol. 9560, pp. 2598–2602, Rome, Italy, 2018.
[18] I. Khoulqi and N. Idrissi, "Cervical Cancer Detection and Classification Using MRIs," Jordanian Journal of Computers and Information Technology (JJCIT), vol. 08, no. 02, pp. 141-158, DOI: 10.5455/jjcit.71-1640595124, June 2022.
[19] D. Azzouz and S. Mazouzi, "A Hyper –surface –based Modelling and Correction of Bias Field in MR Images," Jordanian Journal of Computers and Information Technology (JJCIT), vol. 07, no. 03, pp. 223-238, DOI: 10.5455/jjcit.71-1617051919, Sep. 2021.
[20] H. Sultan, N. Salem and W. Al-Atabany, "Multi-classification of Brain Tumor Images Using Deep Neural Network," IEEE Access, vol. 7, pp. 69215–69225, DOI:10.1109/ACCESS.2019.2919122, 2019.
[21] D. Chen, K. C. Chan and X. Wu, "Gene Expression Analysis Using Genetic Algorithm Based Hybrid Approaches," Proc. of the IEEE Congress on Evolutionary Computation, pp. 963–969, Hong Kong, china, 2008.
[22] Radiopaedia, "Cases," [Online], Available: https://radiopaedia.org/cases/," Accessed on 26 June 2020 .
[23] National Cancer Institute, "Cancer Imaging Archieve," [Online], Available: https://www.cancerimaging archive.net/, Accessed on 30 June 2020.
[24] Biomedical Image Analysis Group, "IXI Dataset," [Online], Available: http://brain-development.org.ixi -dataset, Accessed on 15 June 2020.
[25] K. A. Johnson and J. Alex Becker, "The Whole Brain," Atlas, [Online], Available: http://www.med.harv
ard.edu/AANLIB/, Accessed on 18 June 2021.
[26] Wikipedia, "Confusion Matrix," [Online], Available: http://en.wikipedia.org/wiki/Confusion_matrix, Accessed on 20 Aug 2021.

ملخص البحث:

في هذه الورقة، نقترح إطاراً فعّالاً للاندماج على مستوى السِّمات من أجل تصنيف صُوَر الرّنين المغناطيسي للدّماغ، باستخدام التّعلُّم العميق، واستخلاص السِّمات؛ وبالذّات مخطّط الميول الموجَّهة (HOG)، والأنماط الثّنائية المحلّية (BLPs). ويهدف الإطار المقترح الى: تحديد السِّمات المثالية باستخدام خوارزمية جينية (GA)، واكتشاف سِمات الطّبقات المتّصلة كّلياً باستخدام شبكة عصبية التفافية (CNN) دقيقة الضّبط، وتطبيق التّحليل الارتباطي القانوني (CCA) والتّحليل الارتباطي التّمييزي (DCA) في إحداث الاندماج على مستوى السِّمات.

تم إجراء التّجارب المكثّفة لإظهار مستوى الأداء التّصنيفي للنّظام المقترح على ثلاثةٍ من مجموعات البيانات المرجعية (RD-DB1)، و (TCIA-IXI-DB2)، و (TWB-HM-DB3). وكانت نِسَب الدّقة لمجموعات البيانات المذكورة 68.69%، و 90.35%، و 93.15% على الترتيب عند استخدام تقنية (CCA)، بينما بلغت تلك النِسَب 77.22%، و 100%، و 99.40% على الترتيب عند استخدام تقنية (DCA). ويمكن استنتاج أنّ الإطار المقترح تفوّق على العديد من النّماذج ذات العلاقة المستخدمة في الدّراسات السابقة.